ARTICLES

Effect of Charge Balancing Cations on the Entrapment of CO in Y-Zeolite: FTIR Spectroscopy Study

V. S. Kamble* and N. M. Gupta

Applied Chemistry Division, Bhabha Atomic Research Centre, Trombay, Mumbai 400 085, India

Received: July 14, 1999; In Final Form: March 1, 2000

The effect of charge balancing cations on encapsulation of CO in the pores of Y-zeolite has been investigated using FTIR spectroscopy. The multiple vibrational bands in CO and CO_2 stretching regions, originating from the clusters of these molecules and developed on exposure of CO on Na−Y, undergo an identical shift in frequency and relative intensity when Na^+ are exchanged with group IIA cations. Thus, a constant blue shift of ∼18, 12, and 6 cm^{-1} was observed in all the ν(CO) bands for the samples exchanged with Ca^{2+}, Sr^{2+}, and Ba^{2+}, respectively. The respective $\Delta\nu(CO_2)$ on Ca^{2+}, Sr^{2+}, and Ba^{2+} exchanged zeolite-Y were found to be around +6, +2, and −2 cm^{-1}. The observed frequencies of all the CO and CO_2 vibrational bands and their respective $\Delta\nu$ values with respect to gas-phase frequency are found to show a close relationship with the ionic radius, pore volume, electrostatic potential (e/r), or the field strength (V/Å) associated with the exchanging cations. The data reveal that the characteristics of zeolitic pores play a more important role in encapsulation of CO molecules, rather than the direct bonding of CO at cation sites.

Introduction

In our previous communications we have studied the adsorption of carbon monoxide over X-zeolites by using temperature programmed desorption[1] and infrared spectroscopy[2] techniques. These studies helped us to investigate, respectively, the CO binding states and the formation of $(CO)_n$ molecular clusters entrapped in zeolite super cages on room temperature CO adsorption. It has been demonstrated that the nature of the charge balancing cation had considerable influence on the CO_{ad} species formed during CO adsorption. In recent publications[3,4] we reported on the development of six CO stretching vibrational bands in the 2100−2220 cm^{-1} region during the adsorption of CO in Na−Y and Na-ZSM-5 zeolites at room temperature. In addition, several bands in the 2330−2380 cm^{-1} region due to ν_3 vibration of CO_2 are found to develop in this process. These vibraitonal bands have been attributed to the formation of $(CO)_n$ and $(CO_2)_n$ type molecular clusters encapsulated inside the zeolite cages. In continuation, the effect of exchanging Na^+ with group IIA cations on CO adsorption properties of Na−Y and Na−ZSM5 zeolites have now been investigated using FTIR spectroscopy, and the results for Na−Y are discussed in this paper.

Experimental Section

Na−Y (Si/Al ratio ∼2.7, surface area ∼550 $m^2\ g^{-1}$) was supplied by the Associated Cement Co. Ltd., Thane, India. The template free sample was used after proper washing and drying. Ca^{2+}, Sr^{2+}, and Ba^{2+} exchanged zeolite samples were prepared by the repeated contact of zeolites with 10% nitrate solution of the respective cation at a temperature of ∼335 K and at a pH of about 6. After thorough washing and drying at 400 K, the samples were calcined for 8 h at 720 K under argon flow. The samples were characterized for their crystallinity using the X-ray diffraction (XRD) method (Philips model 1820 powder diffractometer, Cu Kα radiation). Surface area, pore volume, and pore sizes were measured using a Sorptomatic model 1990 analyzer from C. E. Instruments, Rodano (Milan), Italy.

Infrared spectra were recorded in the absorbance mode on a Mattson Cygnus 100 FTIR spectrometer equipped with a DTGS detector. The self-supporting sample wafers (25 mm diameter, 80 mg) were mounted in an IR cell described earlier.[2,5] The samples were heated in situ for about 24 h (at 600 K and ∼1×10^{-4} Torr) before a background spectrum was recorded. CO was then introduced in the cell while the sample wafer was at beam temperature. For each spectrum 300 scans were recorded at a resolution of 4 cm^{-1}. Difference spectra were then obtained by subtracting the IR bands due to residual CO in the cell from the sample spectrum recorded after CO exposure. The spectra given in the text refer to such difference spectra. The values given in parentheses in the figures show the absorbance of individual vibrational bands and indicate their relative intensities. The overlapping spectral bands were resolved using a deconvolution program in the computer software of FTIR.[2−4]

Carbon monoxide of 99.9% purity from AIRCO, New Jersey, was used after proper purification over solidified CO_2.

Results

Characterization. The X-ray diffraction patterns of the exchanged zeolite samples matched with their corresponding sodium form; the typical reflections from the samples containing maximum cation concentration are compiled in Figure 1. No measurable change was observed in the position, relative intensity, or the width of different peaks. The overall peak intensities, however, showed some marginal variations, as is also reported by other workers.[6]

10.1021/jp992400i CCC: $19.00
Published on Web 04/21/2000

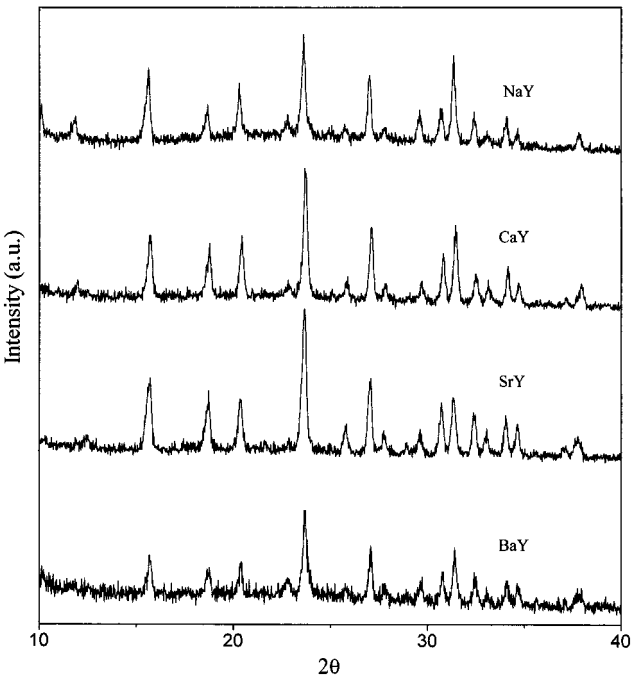

Figure 1. XRD reflections from different cation exchanged Y-zeolites.

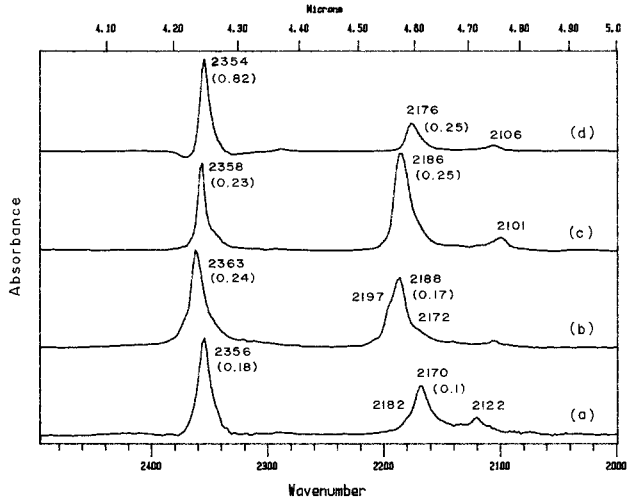

Figure 2. Infrared spectra of Na−Y zeolites exchanged with group IIA cations exposed to 100 Torr of CO at ambient temperature: (a) Na−Y, (b) Ca−Y, (c) Sr−Y, and (d) Ba−Y.

TABLE 1: Specific Surface Area and Pore Volume of Cation Exchanged Y-Zeolites

zeolites	Na−Y	Ca−Y	Sr−Y	Ba−Y
cation exchange (%)		85	82	67
pore vol (cm^3/g)	0.31	0.35	0.33	0.26
surface area (m^2/g)	592	572	558	465

The pore volume of exchanged samples depended on the nature of the charge balancing cation, as shown in the data of Table 1. The pore size was found to be in the range of 9−14 Å irrspective of balancing cation.

CO Adsorption. The exposure of a Na−Y zeolite wafer to carbon monoxide gave rise to multiple vibrational bands in the C−O stretching region, a prominent band appearing at 2170 cm^{-1} (Figure 2a). In addition, several bands in the 2300−2400 cm^{-1} region due to ν_3 vibrations of carbon dioxide were also observed. The intensities of these bands varied with the exposure time, CO pressure, and sample temperature, as has been described earlier.[3] The bands mentioned above shifted in tandem

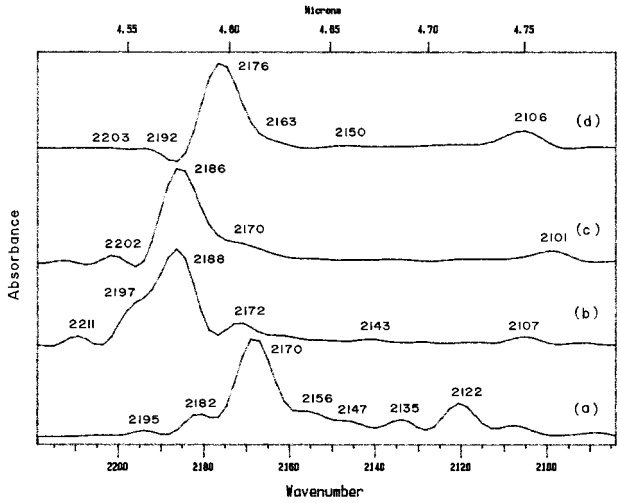

Figure 3. Deconvolution of CO vibrational bands developed on Y-zeolite after exposure to 100 Torr of CO at ambient temperature: (a) Na−Y, (b) Ca−Y, (c) Sr−Y, and (d) Ba−Y.

to higher frequencies on exchange of Na^+ with a group IIA cation. Spectra b−d in Figure 2 show the vibrational bands appearing in CO and CO_2 stretching regions on cation exchanged Y-zeolite samples after exposure to 100 Torr of CO at beam temperature.

Figure 3 presents the Fourier self-deconvolution of ν(CO) region bands, which help in evaluating the changes in individual IR bands as a result of cation exchange. Figure 3a reveals the presence of at least six distinct ν(CO) bands, namely, at 2122, 2135, 2156, 2170, 2182, and 2195 cm^{-1}, developed during the adsorption of CO on Na−Y. A comparison of spectra a−d in Figure 3 shows that the exchange of Na^+ with a group IIA cation results in diminished intensity of some of the weak vibrational bands in the 2110−2140 cm^{-1} region, whereas the intensity of higher frequency bands (i.e., bands at 2156, 2170, 2182, and 2195 cm^{-1} in Figure 3a) increased considerably. Furthermore, data in Figure 3 a−d show the above-mentioned C−O stretch bands shifted uniformly to higher frequencies in the cation exchanged samples, the extent of this shift depending on the nature of the cation. For example, these bands appeared at 2172, 2188, 2197, and 2211 cm^{-1} on Ca−Y (Figure 3b), showing a uniform blue shift of about 16 ± 2 cm^{-1}. In the case of Sr−Y and Ba−Y zeolites this shift is around 15 and 7 cm^{-1}, respectively (Figure 3c,d).

A similar behavior is also observed in case of the vibrational bands in the $\nu_3(CO_2)$ region. Figure 4 presents the deconvolution of these bands for Na−Y, Ca−Y, Sr−Y, and Ba−Y zeolites, appearing after exposure to 100 Torr of CO at beam temperature. These data reveal an identical shift in the frequency of infrared bands observed around 2342, 2356, 2370, and 2382 cm^{-1} in the case of Na−Y (Figure 4a). The value of $\Delta\nu$ is found to be +6 cm^{-1} for Ca−Y (Figure 4b) and around +2 cm^{-1} for Sr−Y zeolite (Figure 4c). In the case of the Ba−Y zeolite sample, these bands show a red shift of −1 to −2 cm^{-1} compared to that of Na−Y (Figure 4d).

The intensity of both the CO and CO_2 stretching bands (indicated by the absorbance value) is relatively higher on cation exchanged samples as compared to Na−Y zeolite. Evacuation of the IR cell after CO exposure at 300 K resulted in the quick removal of all the CO stretching bands from different zeolite samples. The CO_2 stretching band, however, showed a higher stability in the case of cation exchanged samples, which were removed only after evacuation for a longer time or at an elevated temperature. These data are shown in Figure 5.

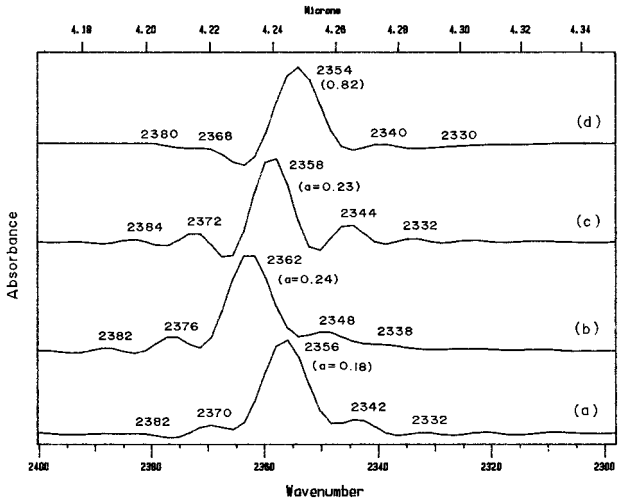

Figure 4. Deconvolution of CO_2 vibrational bands developed on Y-zeolites after exposure to 100 Torr of CO at ambient temperature: (a) Na−Y, (b) Ca−Y, (c) Sr−Y, and (d) Ba−Y.

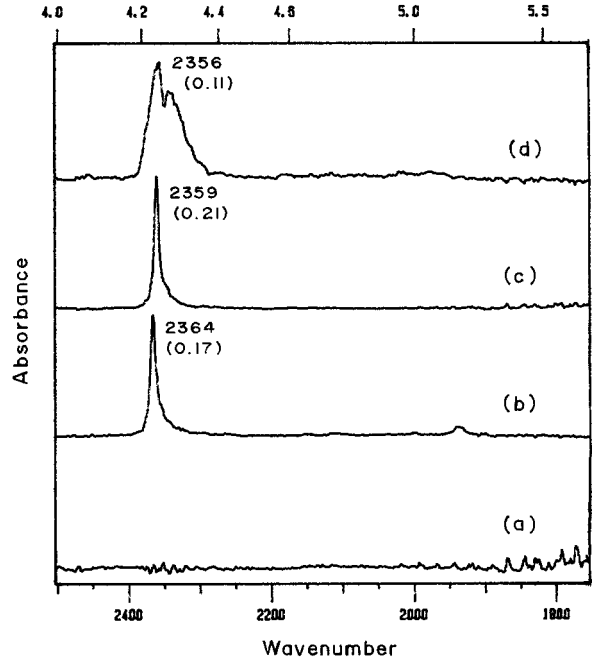

Figure 5. Effect of room temperature evacuation on CO and CO_2 bands formed over cation exchanged Y-zeolites on adsorption of CO at 300 K: (a) Na−Y, (b) Ca−Y, (c) Sr−Y, and (d) Ba−Y.

Effect of Degree of Cation Exchange. The concentration of exchanged cation in Na−Y zeolite had a pronounced effect on the relative intensity of CO and CO_2 stretching bands. For example, the intensity ratio of CO stretch bands at 2188 and 2170 cm^{-1} in the case of Ca−Y zeolite increased with the increasing degree of calcium exchange. Similarly, the intensity ratio of 2182 and 2170 cm^{-1} bands on Sr−Y zeolite increased for a higher degree of Sr^{2+} exchange. The typical CO stretching region spectra obtained on Ca−Y and Sr−Y zeolites, with varying degree of cation exchange and each sample exposed to 100 Torr of CO at ambient temperature, are given in Figure 6A,B, respectively. In these figures, spectra b are obtained with 33% Ca and 28% Sr exchanged samples, while spectra c are obtained with 85% Ca and 82% Sr exchanged zeolites.

Relationship between Frequency and Cation Properties. Parts A and B of Figure 7 show the plots of frequency against the cation field[7−9] for different vibrational bands in the ν(CO) and $\nu_3(CO_2)$ regions. A linear relationship between the field strength and the frequency of associated vibrational bands may be noted in this figure. A parallelism may also be noticed in the plots for different vibrational bands (Figure 7). A linear relationship was also observed when the change in frequency of an individual band was plotted against the pore volume of exchanged zeolite samples (Table 1) or against the electrostatic potential (e/r) or $1/r$, where r is the radius of the exchanged cation. Typical plots showing the frequency−pore volume relationship for some of the prominent ν(CO) bands are given in Figure 7C.

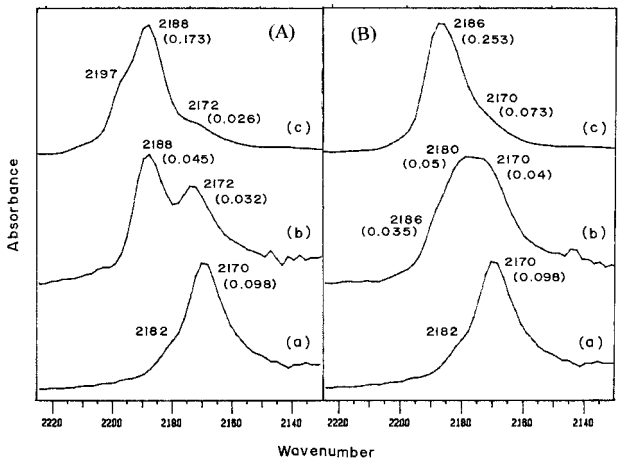

Figure 6. Effect of Ca^{2+} and Sr^{2+} concentrations on the relative intensities of different ν(CO) vibrational bands developed on zeolites-Y after exposure to 100 Torr of CO at ambient temperature: for A, (a) Na−Y, (b) Ca(33%)−Y, and (c) Ca(85%)−Y; for B, (a) Na−Y, (b) Sr(28%)−Y and (c) Sr(82%)−Y.

Discussion

Infrared spectroscopy has been widely employed to investigate the mode of CO bonding in zeolites. The nature and the position of IR bands thus developed are shown to depend on various factors, such as sample temperature, adsorbate pressure, the nature of the zeolite, and the charge balancing cation.[9−11] Zeolitic sites, such as surface hydroxy groups,[15,17] aluminum sites,[10,14,19,20] and the charge balancing cations,[9,11−14,18,20,21] are reported to be the centers involved jointly or separately in CO bonding. Bonding of CO to cations through both C and O atoms has been proposed. In a recent study on ZSM5 zeolite, Otero Arean et al.[22] suggested the existence of an equilibrium between C-bonded and O-bonded adducts, i.e., $Z-Na^{+}\cdots CO \rightleftharpoons Z-Na^{+}\cdots OC$, where Z represents the zeolitic framework.

Most of the above-mentioned studies, however, pertain to the experiments performed at low temperatures, i.e., 77 K. In recent publications, we reported our IR investigation of CO adsorption over Y- and ZSM-5-zeolites at temperatures in the range 300−473 K and at pressures of 10−500 Torr.[3,4] Our studies revealed that the intensity and the frequency of different vibrational bands, due both to CO and CO_2 stretchings, show monotonic changes on evacuation, temperature rise, and increase in adsorbate pressure and also on using the isotopically labeled carbon monoxide. On the basis of these results, we inferred that the vibrational bands in the ν(CO) and $\nu_3(CO_2)$ regions may not originate from the bonding of CO with specific zeolite sites, i.e., charge balancing cations or framework Bronsted and Lewis acid sites. This led us to conclude that the adsorption of CO resulted in its encapsulation within zeolite cages in the form of $(CO)_n$ and $(CO_2)_n$ molecular clusters. Possible routes giving rise to CO_2 formation in zeolite cages have also been discussed in our previous papers.[3,4]

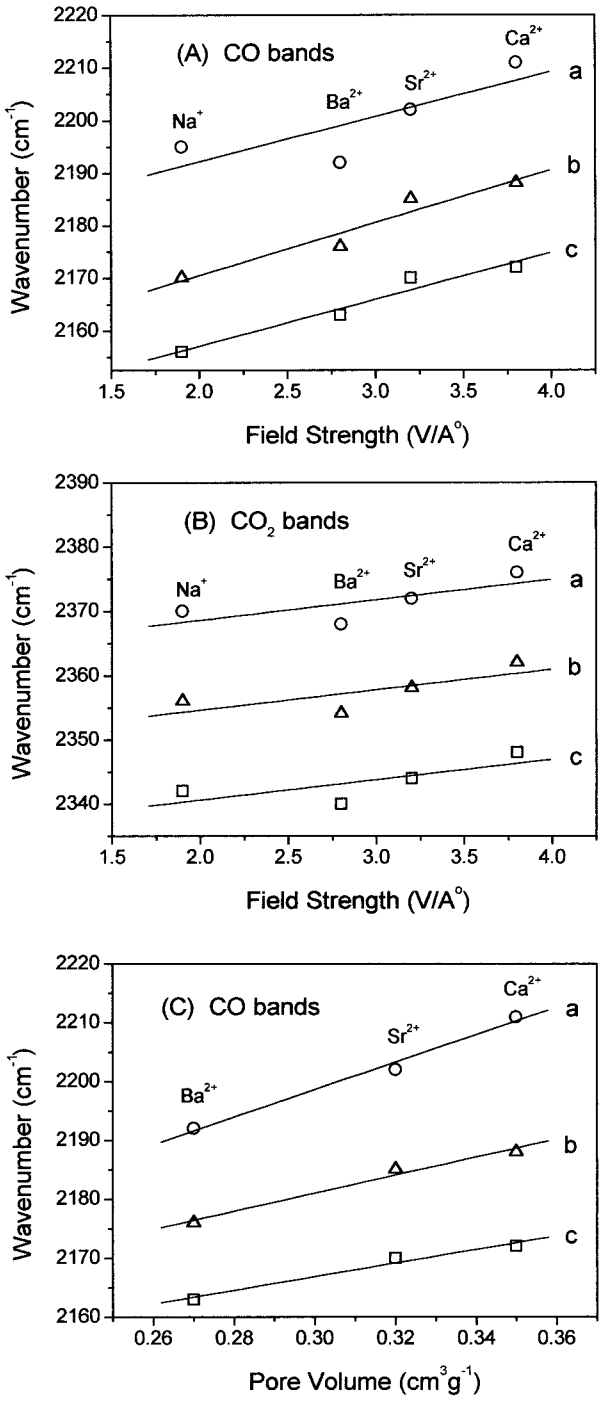

Figure 7. Plot of ν(CO) and $\nu(CO_2)$ frequencies against the electrostatic field associated with a cation and the pore volume of different cation exchanged Y-zeolites.

Data in Figure 7 reveal a strong correlation between the observed shift in the frequency of individual bands formed on the adsorption of CO over cation exchanged samples (Figures 3 and 4) and the physical parameters such as the field strength or *e*/*r* ratio associated with the exchanging cation. Such a correlation has been reported in the earlier publications also.[7,11,12] On the basis of this relationship, it is believed that the charge balancing cations are directly involved in the entrapment or bonding of CO in zeolitic cages. We may however point out that the S_I sites located at the center of the hexagonal prisms and S_{II} sites located in the sodalite cages are the most preferred sites for bivalent cations; but these sites are known to be inaccessible to molecules such as CO or CO_2. Thus, the sites where the bonding of CO may occur could be identified as the S_I' and S_{II}' sites in the super cages of Y-zeolite. In view of this, the bonding of CO at a few localized cation sites is unlikely to result in an identical frequency shift in all the vibrational bands, both in partially and fully exchanged samples (Figures 3 and 6). These aspects have been discussed earlier in more detail.[3] We can similarly infer that a monotonic frequency shift in ν-(CO_2) bands as seen in Figure 4 can also not arise from the direct bonding of individual or cluster molecules of carbon dioxide at the specific cation sites.

We therefore turn to an alternative explanation based on the observed relationship between the pore volume, which depends on the cation radius (Table 1) and the frequency of the vibrational bands (Figure 7c). Figure 1 shows that there is no significant shift in the position of XRD peaks on exchanging Na^+ with a group IIA cation. This indicates that the symmetry of zeolite does not change with the size of the cation, and the zeolite structure remains undistorted. Therefore, the only effect of countercation is an increase in density and a decrease in pore volume of both the sodalite and super cages. This inference is based on an increase in mass and ionic radius without causing an expansion or distortion of the unit cell on going from Ca^{2+} to Ba^{2+}. This is further supported by the data of Table 1. A similar trend in the change of pore volume with cation substitution in X-zeolite has been reported.[23]

In consonance with our molecular cluster model,[2−4] the shift in the frequency of IR bands in Figures 2−6 may thus be explained as follows. The increase in pore volume will lead to a decreased dipole−dipole interaction between two CO molecules of a dimer and hence in lengthening of the C−C bond distance in a O≡C---C≡O cluster.[3,4] This will consequently result in the greater charge concentration (bond strength) of the C≡O bond, leading thereby to a positive frequency shift in ν(CO) bands, as is observed in our study (Figure 3). The extent of this shift will depend on the change in pore volume, as is also observed (Figure 7C).

The results of Figure 6 show that with a change in cation content from about 30 to 85% the ratio of the intensities of the CO stretching vibrational bands associated with M^{2+} and Na^+ increases from 1.4 to 6.65 for Ca−Y zeolite and from 1.25 to 3.47 for Sr−Y zeolite. These data point to the existence of the cavities of at least two distinct volumes in a partially exchanged zeolite, one where substitution of the cation has taken place and the other where it has not. The encapsulated clusters of CO may give rise to distinct vibrational bands depending on the cavity characteristics, as observed in Figure 6.

It is reported[24,25] that the multivalent cations in the S_I positions of zeolite-Y migrate during calcination, thus reducing the diameter of the six membered ring (window opening for α cage) in the hexagonal prism. The slower release of larger $(CO_2)_n$ clusters during the postexposure evacuation (Figure 5) may thus be attributed to such pore restrictions in cation exchanged samples.

We may thus conclude that the CO or CO_2 molecules entrapped in narrow zeolitic cages experience a dipole−dipole or van der Waals type weak interaction and resultantly exist in the form of $(CO)_n$ and $(CO_2)_n$ clusters. The dimensions of cavities cast considerable influence on the intermolecular distance in these clusters, which in turn is reflected clearly in their IR spectra.

Acknowledgment. We thank Dr. A. K. Tyagi for his help in the XRD analysis and for discussions. Discussions with Dr.

V. B. Kartha, MAHE, Manipal, India, are also gratefully acknowledged.

References and Notes

(1) Gupta, N. M.; Kamble, V. S.; Rao, K. A.; Iyer, R. M. *J. Catal*. **1989**, *120*, 432.

(2) Kamble, V. S.; Gupta, N. M.; Kartha, V. B.; Iyer, R. M. *J. Chem. Soc., Faraday Trans*. **1993**, *89*, 1143.

(3) Shete, B. S.; Kamble, V. S.; Gupta, N..M.; Kartha, V. B. *J. Phys. Chem. B* **1998**, *102*, 5581.

(4) Shete, B. S.; Kamble, V. S.; Gupta, N. M.; Kartha, V. B. *Phys. Chem. Chem. Phys*. **1999**, *1*, 191.

(5) Kamble, V. S.; Gupta, N. M.; Iyer, R. M. *Ind. J. Chem*. **1990**, *29A*, 1089.

(6) Kanno, Y.; Imai, H. *Mater. Res. Bull*. **1982**, *17*, 1161.

(7) Rabo, J. A.; Angel, C. L.; Kasai, P. H.; Schomaker, V. *Discuss. Faraday Soc*. **1966**, *41*, 328.

(8) Ward, J. W. *J. Catal*. **1968**, *10*, 34.

(9) Zecchina, A.; Bordiga, S.; Lamberti, C.; Spoto, G.; Carnelli, L.; Otero Areán, C. *J. Phys. Chem*. **1994**, *98*, 9577.

(10) Zecchina, A.; Escalona Platero, E.; Otero Areán, C. *J. Catal*. **1987**, *107*, 244.

(11) Bordiga, S.; Scarano, D.; Spoto, G.; Zecchina, A.; Lamberti, C.; Otero Areán, C. *Vib. Spectrosc*. **1993**, *5*, 69.

(12) Angell, C. L.; Schaffer, P. C. *J. Phys. Chem*. **1966**, *70*, 1413.

(13) Gruver, V.; Fripiat, J. J. *J. Phys. Chem*. **1994**, *98*, 8549.

(14) Chem, L.; Lin, L.; Xu, Z.; Zhang, T.; Xim, Q.; Ying, P.; Li, G.; Li, C. *J. Catal*. **1996**, *161*, 107.

(15) Bordiga, S.; Escalona Platero, E.; Otero Areán, C.; Lamberti, C.; Zecchina, A. *J. Catal*. **1992**, *137*, 179.

(16) Neyman, K. M.; Stradel, P.; Ruzankin, S. P.; Schlensog, N.; Knözinger, H.; Rösch, N. *Catal. Lett*. **1995**, *31*, 272.

(17) Kustov, L. M.; Kazansky, V. B.; Beran S.; Kubelkova, L.; Jiru, P. *J. Phys. Chem*. **1987**, *91*, 5247.

(18) Turnes Palomino, G.; Otero Areán, C.; Geobaldo, F.; Ricchiardi, G.; Bordigia, S.; Zecchina, A. *J. Chem. Soc., Faraday Trans*. **1997**, *93*, 189.

(19) Zaki, M.; Knözinger, H. *Spectrochim. Acta A* **1987**, *43*, 1455.

(20) Zecchina, A.; Otero Areán, C. *Chem. Soc. Rev*. **1996**, *25*, 187.

(21) Egerton, T. A.; Stone, F. S. *J. Chem. Soc., Faraday Trans 1* **1987**, *69*, 22.

(22) Otero Areán, C.; Tsyganenko, A. A.; Escalona Platero, E.; Garrone, E.; Zecchina, A. *Angew Chem., Int. Ed. Engl*. **1998**, *37*, 3161.

(23) Zhang, S.-Y.; Talu, O.; Hayhurst, D. T. *J. Phys. Chem*. **1991**, *95*, 1722.

(24) Rees, L. V. C. *Annu. Rep. Prog. Chem*. **1970**, 191.

(25) Bennett, J. M.; Smith, J. V. *Mater. Res. Bull*. **1968**, *3*, 623.